

Electronic Supplementary Information

Mesoporous Polyoxometalate Cluster–Crosslinked
Organosilica Frameworks Delivering Exceptionally High
Photocatalytic Activity

Eirini D. Koutsouroubi, Alexandra K. Xylouri and Gerasimos S. Armatas*

Materials Science and Technology, University of Crete, Heraklion 71003, Crete, Greece.

E-mail: garmatas@materials.uoc.gr

Experimental section

Pluronic P123 surfactant ($\text{HO}(\text{CH}_2\text{CH}_2\text{O})_{20}(\text{CH}_2\text{CH}(\text{CH}_3)\text{O})_{70}(\text{CH}_2\text{CH}_2\text{O})_{20}\text{H}$, $M_n \sim 5800$), 1,2-bis(triethoxysilyl)ethane ($\geq 96\%$), absolute ethanol (99.8%), tetramethylammonium chloride ($\text{N}(\text{CH}_3)_4\text{Cl}$, 98%), dimethyl sulfoxide ($\geq 99.9\%$) were purchased from Sigma-Aldrich. Hydrochloric acid solution (1M) was purchased from Merck. Sodium tungstate ($\text{Na}_2\text{WO}_4 \cdot 2\text{H}_2\text{O}$, 99%) and sodium metasilicate ($\text{Na}_2\text{SiO}_3 \cdot 9\text{H}_2\text{O}$, 98%) were purchased from Alfa-Aesar. The 1-phenylethanol and benzyl alcohols used as substrates were of high purity and commercially available from Sigma-Aldrich.

Synthesis of polyoxometalate $[\alpha\text{-SiW}_{11}\text{O}_{39}]^{8-}$

Mono lacunary silicotungstates $\text{K}_8[\alpha\text{-SiW}_{11}\text{O}_{39}]$ and $(\text{NBu}_4)_8[\alpha\text{-SiW}_{11}\text{O}_{39}]$ were prepared according to the literature procedure.¹

Synthesis of organically-modified silicotungstate

The hybrid $[\text{SiW}_{11}\text{O}_{39}\{\text{O}(\text{Si}(\text{OH})_2\text{C}_2\text{H}_4\text{Si}(\text{OH})_3)_2\}]^{4-}$ polyoxometalate (POM) (denoted as $\text{SiW}_{11}(\text{SiOH})_2^{4-}$) was prepared by following a similar procedure reported previously.² Briefly, 2 g of $\text{K}_8\text{SiW}_{11}\text{O}_{39}$ was dissolved in 50 mL of deionized water under stirring. Then, 0.437 mL of 1,2-bis(triethoxysilyl)ethane (BTSE) was added dropwise and the pH of solution was adjusted to 1 with 1 M HCl. The resulting mixture was stirred for about 20 h at room temperature to obtain a clear solution. Consequently, the solution was concentrated under reduced pressure in a rotary evaporator to get a white precipitate. This solid was dissolved in 25 mL of water, and then filtered on a glass frit (no. 4). Tetramethylammonium salt of the target compound, $(\text{NMe}_4)_4\text{SiW}_{11}(\text{SiOH})_2$, was obtained by adding excess of $\text{N}(\text{CH}_3)_4\text{Cl}$ (0.276 g) and the white microcrystals (1.7 g, 71%) was collected by filtration, washed with 2-propanol and dried under vacuum at 40 °C. This compound was characterized by IR spectroscopy (IR (KBr) ν 2961, 2936, 2874, 1485, 1042, 948, 907, 798, 533 cm^{-1} , Fig. S4).

Synthesis of mesoporous $\text{SiW}_{11}/\text{MES}$ hybrid materials

In a typical experiment, 1 g of Pluronic P123 triblock copolymer was dissolved in 12 mL of deionized water. In a separate vial, 5.16 mmol of BTSE was slowly added to a mixture containing 12 mL deionized water and 2.5 mL 1 M HCl. The two solutions were then mixed together under continuous stirring at 40 °C. After 5 min, a clear solution of $(\text{NMe}_4)_4\text{SiW}_{11}(\text{SiOH})_2$ POM in 5 mL dimethyl sulfoxide (DMSO) was added to the reaction solution and the resulting mixture was stirred vigorously at 40 °C for about 24 h. The mixture was then placed in a Teflon-lined autoclave and heated in an oven at 100 °C for 5 days. The white precipitate was collected by filtration, subsequently washed with water and ethanol and dried at 60 °C. Template removal was achieved by ethanol extraction of the as-made (containing surfactant) materials at 70 °C for 6 h.³

Mesoporous materials with different loading amount of $[\text{SiW}_{11}\text{O}_{39}]^{n-}$ (SiW_{11}) clusters were prepared following the above method, varying the amount of the functionalized $(\text{NMe}_4)_4\text{SiW}_{11}(\text{SiOH})_2$ POMs. The amount of POM used in reactions was varied between 33, 52 and 125 μmol to give a series of mesoporous $\text{SiW}_{11}/\text{MES}$ hybrid materials with ~ 9 , ~ 15 and $\sim 25\%$ (w/w) $[\text{SiW}_{11}\text{O}_{39}]^{n-}$ loading, as determined by elemental EDS analysis. The EDS POM contents are slightly lower than those expected from the stoichiometry of reactions, i.e. 10, 15 and 30% (w/w). Mesoporous ethane-silica (denoted as MES) was prepared in a similar procedure to $\text{SiW}_{11}/\text{MES}$, but without addition of POM.

Characterization

The small angle XRD patterns were collected using a PANalytical X'pert Pro MPD X-ray diffractometer equipped with a Cu ($\lambda=1.5418 \text{ \AA}$) rotating anode operated at 40 mA and 45 kV, in the Bragg-Brentano geometry.

Nitrogen adsorption-desorption isotherms were measured at 77 K using liquid N₂ on a Quantachrome Model NOVA 3200e sorption analyzer. Before analysis, samples were degassed overnight at 373 K under vacuum ($<10^{-4}$ mbar). The specific surface areas were calculated using the Brunauer-Emmett-Teller (BET) method on the adsorption data in the 0.05–0.24 relative pressure (P/P_0) region. The total pore volumes were estimated from the adsorbed amount at the $P/P_0 = 0.98$ and the pore size distributions were obtained from the adsorption data using the nonlocal density functional theory (NLDFT) method.

Transmission electron microscopy (TEM) images were taken with a JEOL Model JEM-2100 electron microscope operating at 200 kV accelerated voltage. The samples were first gently ground, ultrasonically dispersed in ethanol, and then picked up on a holey carbon-coated Cu grid.

Elemental microprobe analyses were performed using a JEOL Model JSM-6390LV scanning electron microscope (SEM) equipped with an Oxford INCA PentaFETx3 energy dispersive X-ray spectroscopy (EDS) detector. Samples were gently placed on carbon tape, forming flat surfaces, and taken into the instrument chamber for analysis. Data acquisition was performed several times in different areas of samples using an accelerating voltage of 20 kV and 100-s accumulation time.

Thermogravimetric analyses (TGA) were performed on a Perkin-Elmer Diamond system. Thermal analysis was conducted from 40 to 600 °C in air atmosphere (100 mL min⁻¹ flow rate) with a heating rate of 5 °C min⁻¹.

Infrared (IR) spectra were recorded on a Perkin Elmer Model Frontier FT-IR spectrometer with 2 cm⁻¹ resolution. Samples were prepared as KBr pellets.

Raman spectra were recorded at room temperature on a Nicolet Almega XR micro-Raman spectrometer equipped with a 473 nm blue laser (15 mW) as an excitation source.

Diffuse reflectance UV/vis spectra were obtained on a Perkin-Elmer Lambda 950 optical spectrophotometer, using an integrating sphere. BaSO₄ powder was used as a 100% reflectance standard. The reflectance data were converted to absorption using the Kubelka–Munk equation: $a/S = (1-R)^2/(2R)$, where R is the reflectance and a and S are the absorption and scattering factors, respectively.

Catalytic reactions

The photocatalytic reactions were carried out in a 4-mL vial equipped with a PTFE cap. In the vial, 0.1 mmol of substrate and appropriate amount of catalyst (3 μ mol catalyst, based on SiW₁₁ loading) were added in 2 mL of α,α,α -trifluorotoluene. The reaction mixture was first stirred in the dark for 30 min to homogeneously disperse the catalyst in the solution. The reaction was initiated by irradiation with a Variac Cermax 300 W Xe Lamp ($\lambda>360$ nm). During irradiation, the reaction mixture was bubbled with oxygen (~ 15 mL min⁻¹) and cooled with a water bath (20 \pm 2 °C). Product analysis was performed on a Shimadzu GC-MS QP2010 Ultra system equipped with a 60 m Mega-5 MS capillary column, using He as carrier gas. Blank experiments in the absence of catalyst or UV irradiation did not show any catalytic activity.

For recycling experiments, the photocatalyst was recovered by centrifugation, washed with α,α,α -trifluorotoluene, dried under vacuum at 80 °C, and used for the next catalytic run.

Table S1 Morphological properties of mesoporous ethane-silica (MES) and $x\%$ SiW₁₁/MES materials.

Sample	d -spacing (nm)	BET Surface area (m ² g ⁻¹)	Pore volume (cm ³ g ⁻¹)	Pore size (nm)
MES	10.4	978	1.24	8.3
9% SiW ₁₁ /MES	12.1	962	1.28	7.8
15% SiW ₁₁ /MES	12.3	867	1.19	7.8
25% SiW ₁₁ /MES	12.6	725	1.04	7.7

Table S2. Catalytic activities of various SiW₁₁-containing catalysts for the photooxidation of 1-phenylethanol to acetophenone with molecular O₂.^a

Catalyst	Yield (%) ^b	Kinetic constant ^c , <i>k</i> (min ⁻¹)
9% SiW ₁₁ /MES	24	0.004
15% SiW ₁₁ /MES	73	0.020
25% SiW ₁₁ /MES	57	0.012
(NBu ₄) ₈ [SiW ₁₁ O ₃₉]	5 ^d	-

^aReaction conditions: 0.1 mmol 1-phenylethanol, 3 μmol catalyst (based on SiW₁₁ loading), 2 mL α,α,α-trifluorotoluene, O₂ bubbling (~15 mL min⁻¹), 20 °C, UV light irradiation (λ>360 nm). ^bYield at 1 h, determined by GC-MS analysis, with error ±1%. ^cReaction rate constant (*k*) assuming pseudo-first-order kinetics. ^dAt 4 h irradiation time.

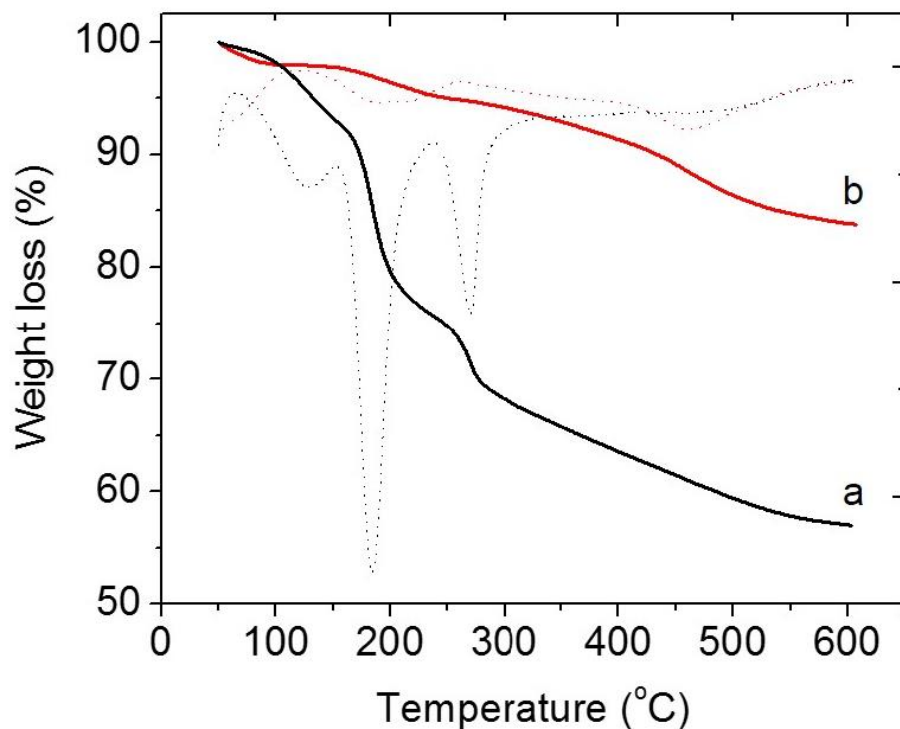


Fig. S1 TGA profiles (solid lines) performed in air and the corresponding differential thermogravimetric (DTG) curves (dashed lines) of (a) as-prepared containing surfactant and (b) ethanol-extracted mesoporous 15% SiW₁₁/MES sample.

The TGA profile of as-prepared (containing surfactant) sample shows a weight loss in the temperature range 50–150 °C due to the liberation of physisorbed solvent. The weight loss (~29%) observed between 150 and 350 °C, which is accompanied by at least two-step process as indicated by the DTG curve, is attributed to the decomposition of surfactant. The TGA profile of ethanol-extracted sample show a ~5.1% weight loss between 150 and 360 °C, which corresponds mainly to the decomposition of surfactant residue in the pores. This process is followed by a gradual weight loss at temperatures between 400 and 600 °C, which correspond to the loss of ethane fragment in silsesquioxane component.

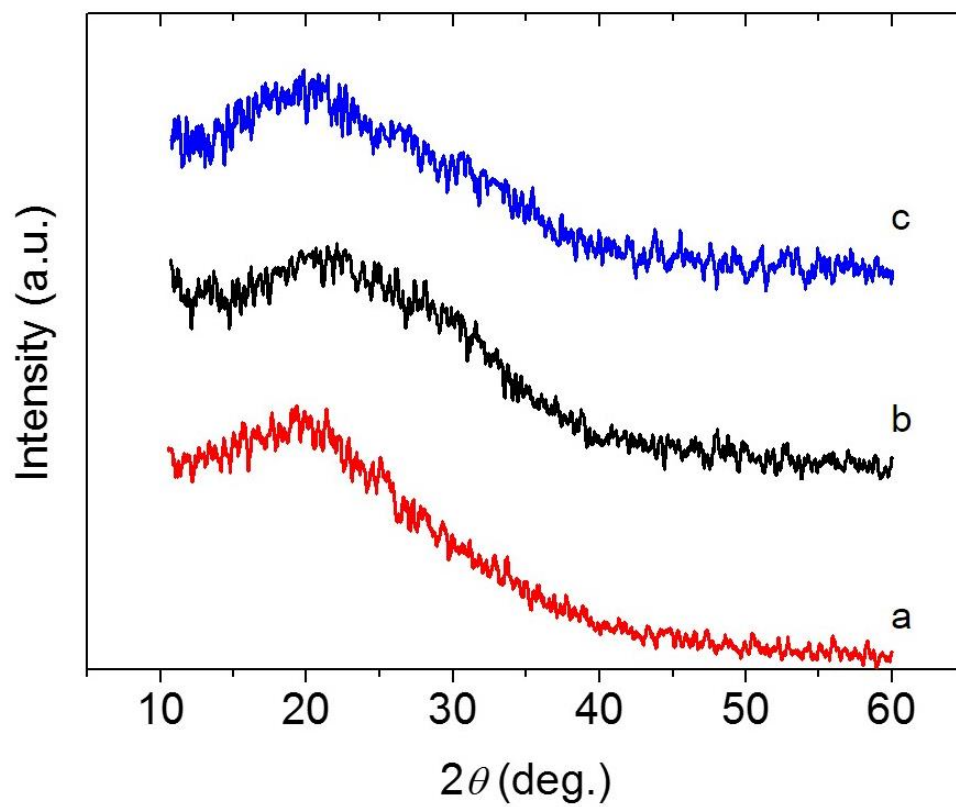


Fig. S2 Wide-angle XRD patterns of mesoporous hybrid SiW₁₁/MES polymers containing (a) 9, (b) 15 and (c) 25% (w/w) SiW₁₁ loading.

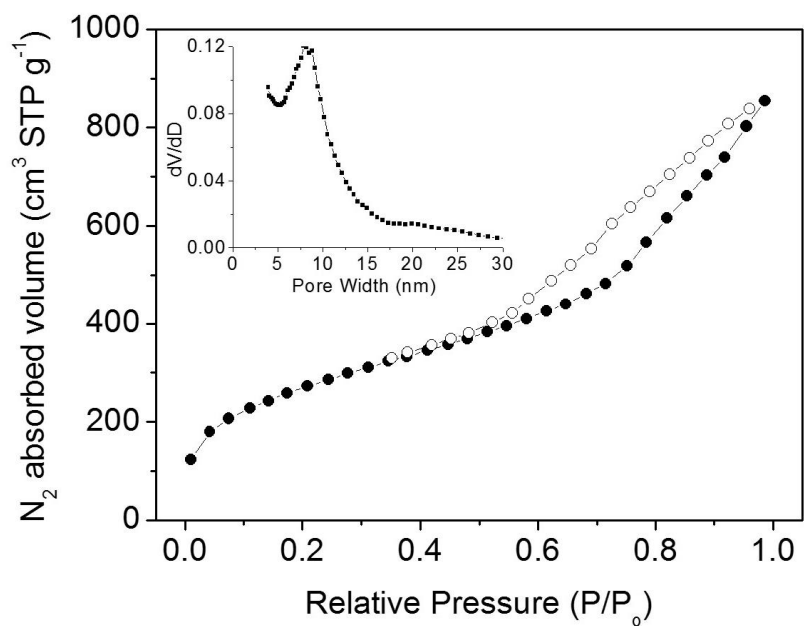


Fig. S3 N₂ adsorption-desorption isotherms at 77 K and the corresponding NLDFT pore size distributions calculated from the adsorption data (inset) for mesoporous ethane-silica (MES) material.

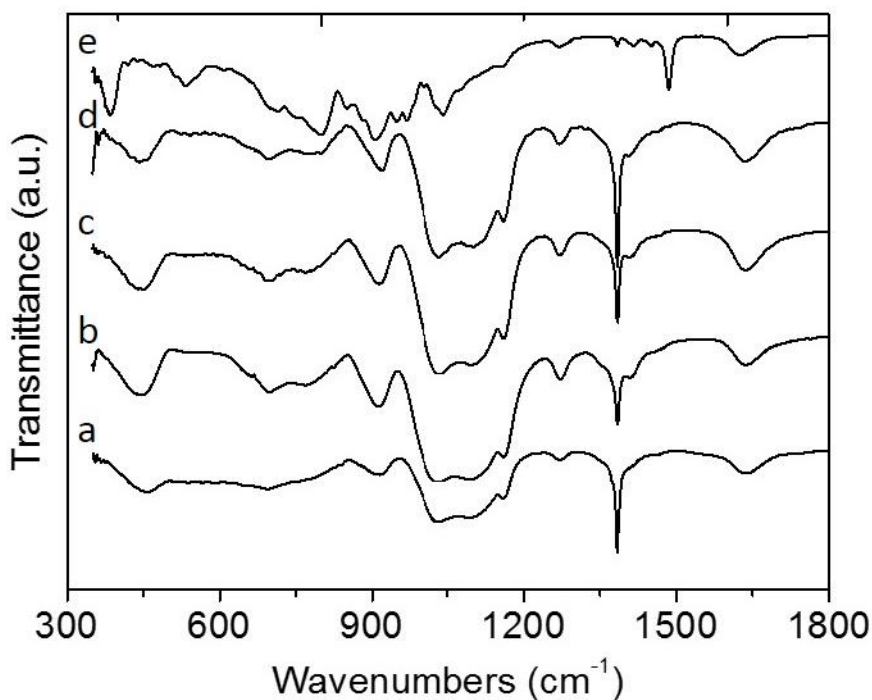


Fig. S4 Infrared spectra of mesoporous (a) ethane-silica (MES) and (b) 9%, (c) 15% and (d) 25% (w/w) SiW_{11} -loaded ethane-silica ($\text{SiW}_{11}/\text{MES}$) polymeric materials and (e) hybrid $(\text{NMe}_4)_4\text{SiW}_{11}(\text{SiOH})_2$ compound.

The IR spectrum of mesoporous ethane-silica (MES) material shows intense absorption peaks at 1385 and 1270 cm^{-1} , $1030\text{--}1033\text{ cm}^{-1}$ and $1100\text{--}1108\text{ cm}^{-1}$, which are attributed to the vibration bands of $-\text{CH}_2$ groups, the stretching vibration of Si-O-Si bond and the stretching vibration of Si-O-C bond, respectively, of the silsesquioxane framework. The peaks at 1163 and 1103 cm^{-1} are attributed to the stretching vibrations of O-C and Si-O-C bonds, respectively. The absorption peak at 912 cm^{-1} can be assigned to the bending vibration band of Si-O-Si bond.[15] The IR spectra of $x\%$ $\text{SiW}_{11}/\text{MES}$ polymers show also the characteristic stretching vibration bands of the Keggin $[\text{SiW}_{11}\text{O}_{39}]^{12-}$ clusters: (1) the W=O_d asymmetrical stretching vibration at $914\text{--}922\text{ cm}^{-1}$, (2) the W-O-W asymmetrical stretching band at 780 cm^{-1} , and (3) the W-O-W symmetrical stretching band in the $530\text{--}536\text{ cm}^{-1}$ region.[14] The organically-modified $(\text{NMe}_4)_4\text{SiW}_{11}(\text{SiOH})_2$ complex exhibits the W=O_d stretching band in the $907\text{--}948\text{ cm}^{-1}$ region and the W-O-W asymmetrical and symmetrical stretching vibration bands at ~ 798 and $\sim 533\text{ cm}^{-1}$, respectively. On the hybrid POM the absorption peak at 1042 cm^{-1} is attributed to the stretching vibration of Si-O bonds and the intense peak at 1485 cm^{-1} is assigned to the methyl $(-\text{CH}_3)$ asymmetric bending mode of $\text{N}(\text{CH}_3)_4^+$ cations.

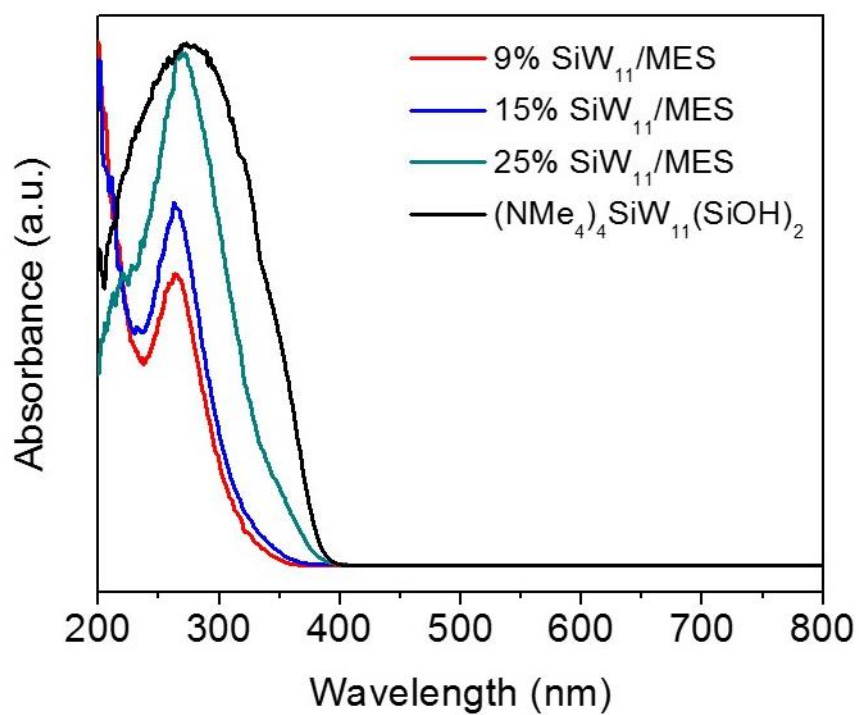


Fig. S5 Diffuse reflectance UV-vis spectra of mesoporous ethane-silica (MES) and $x\%$ SiW₁₁/MES materials and (NMe₄)₄SiW₁₁(SiOH)₂ complex.

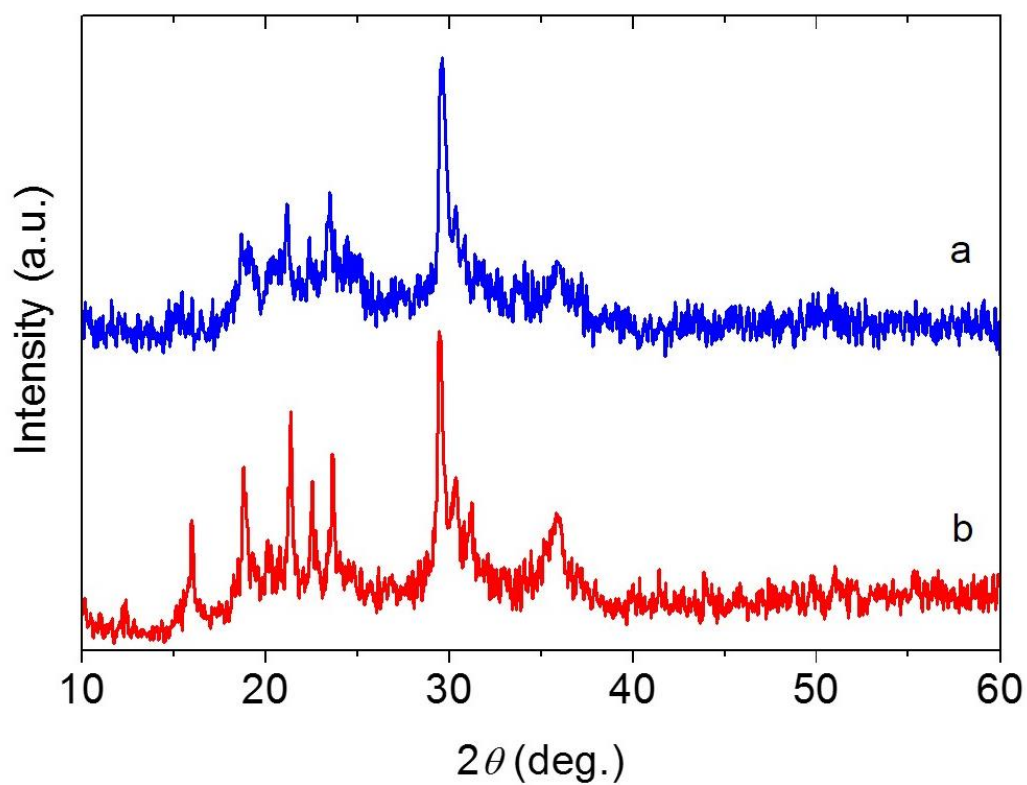


Fig. S6 X-ray diffraction patterns of (a) NBu_4^+ precipitate obtained after dissolution of the 15% $\text{SiW}_{11}/\text{MES}$ sample with HF (5% by weight in water) and (b) as-prepared $(\text{NBu}_4)_8[\text{SiW}_{11}\text{O}_{39}]$ compound.

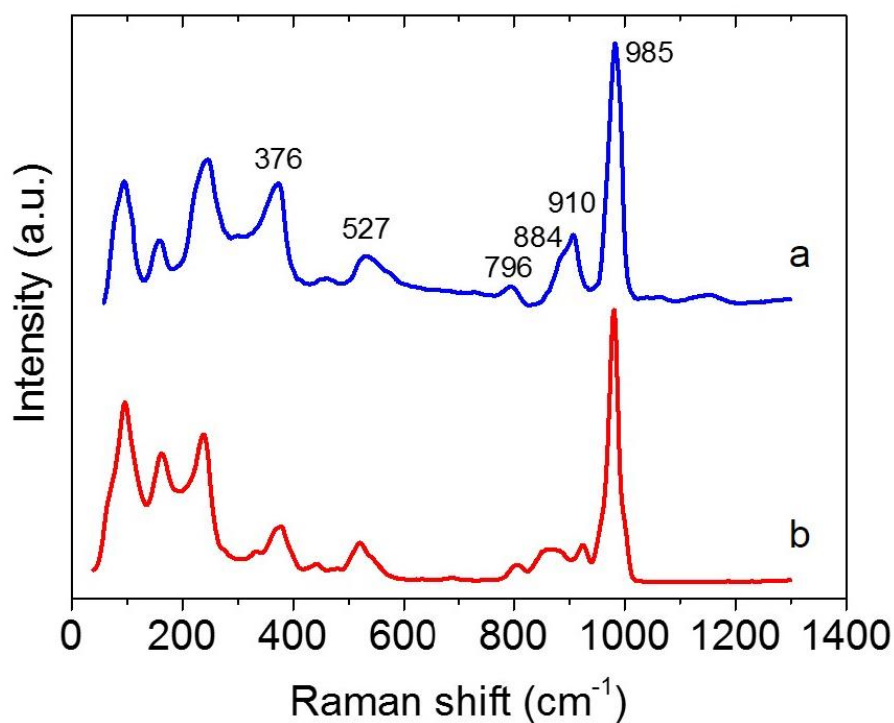


Fig. S7 Raman spectra of (a) NBu_4^+ precipitate obtained after dissolution of the 15% $\text{SiW}_{11}/\text{MES}$ sample with HF and (b) as-prepared $(\text{NBu}_4)_8[\text{SiW}_{11}\text{O}_{39}]$ compound.

The Raman spectra of NBu_4^+ precipitate obtained after dissolution of the 15% $\text{SiW}_{11}/\text{MES}$ polymer in hydrofluoric acid and $(\text{NBu}_4)_8[\text{SiW}_{11}\text{O}_{39}]$ compound show intense peaks in $900\text{--}1000\text{ cm}^{-1}$ region that correspond to the $\text{W}=\text{O}_d$ stretching mode and two weak features between 790 and 890 cm^{-1} due to the asymmetric stretching modes of $\text{W}\text{--}\text{O}\text{--}\text{W}$ bonds in the lacunary $\alpha\text{-}[\text{SiW}_{11}\text{O}_{39}]^{8-}$ cluster, respectively.⁴ The Raman shifts at ~ 527 and $\sim 376\text{ cm}^{-1}$ are associated with the bending modes of $\text{W}\text{--}\text{O}\text{--}\text{W}$ and $\text{O}\text{--}\text{Si}\text{--}\text{O}$ bonds.

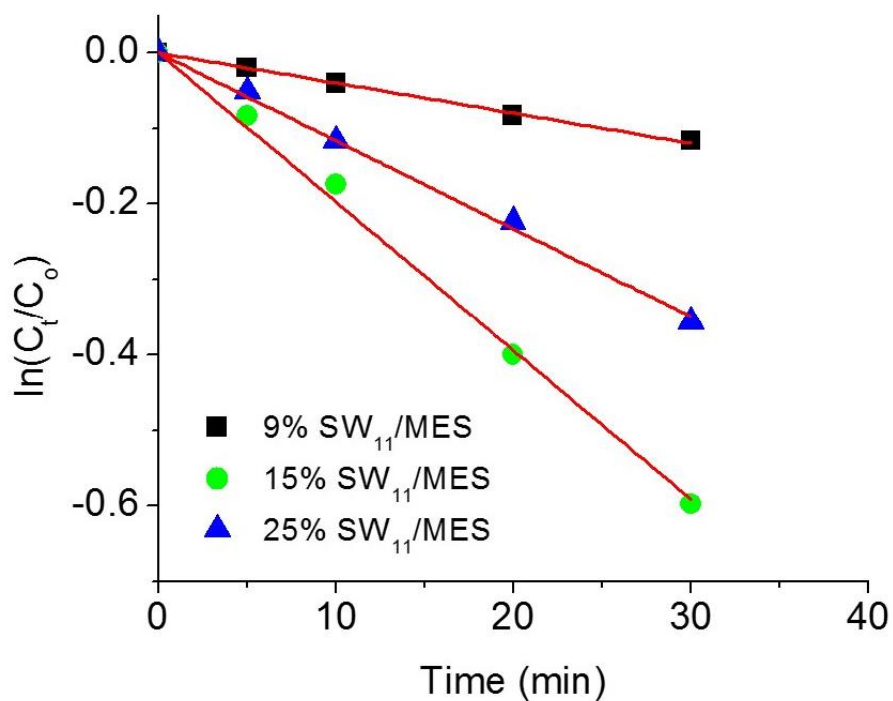


Fig. S8 The pseudo first-order rate plots (C_0 , C_t are the initial and final (at time t) concentrations of 1-phenylethanol, respectively) for the photooxidation of 1-phenylethanol catalyzed by various mesoporous ethane-silica materials ($x\%$ SW₁₁/MES) loaded with different amounts of SiW₁₁. The corresponding red lines are fit to the data.

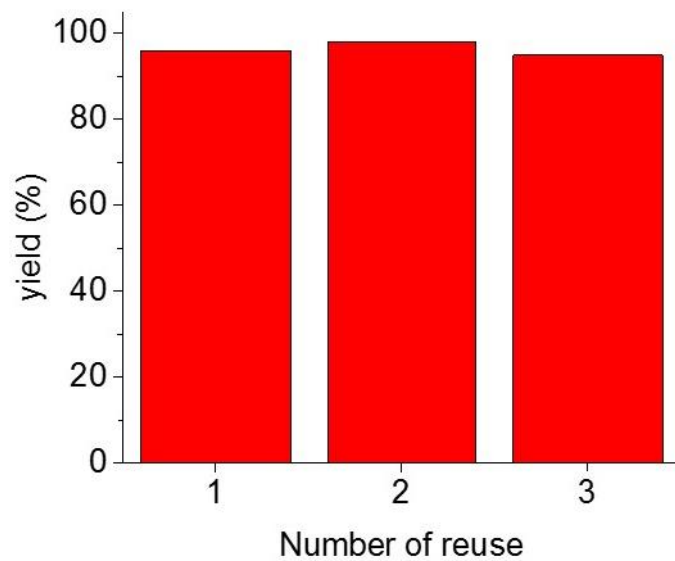


Fig. S9 Recycling study of the mesoporous 15% SW₁₁/MES catalyst. *Reaction conditions:* 0.1 mmol 1-phenylethanol, 3 μ mol catalyst (based on SiW₁₁ loading), 2 mL α,α,α -trifluorotoluene, O₂ bubbling (\sim 15 mL min⁻¹), 20 °C, UV light irradiation ($\lambda > 360$ nm), 2 h.

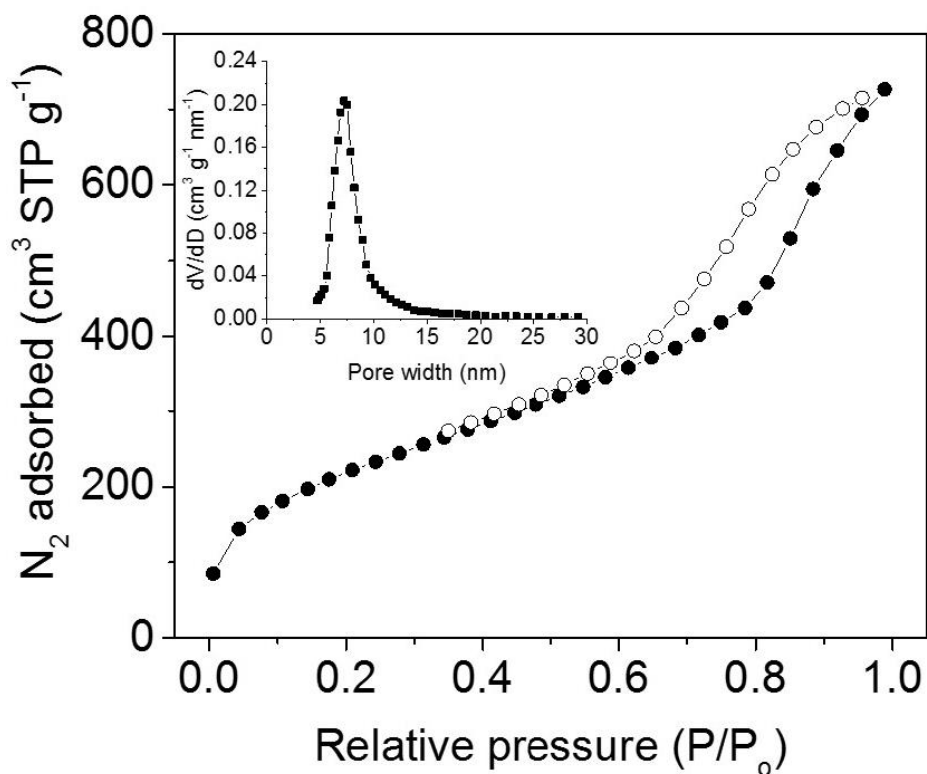


Fig. S10 Nitrogen adsorption–desorption isotherms at 77 K of three-times reused 15% SW₁₁/MES catalyst. BET analysis on adsorption data indicates a surface area of 814 m²g⁻¹ and total pore volume of 1.09 cm³g⁻¹. Inset: the corresponding NLDFT pore size distribution indicating a pore diameter of ~ 7.5 nm.

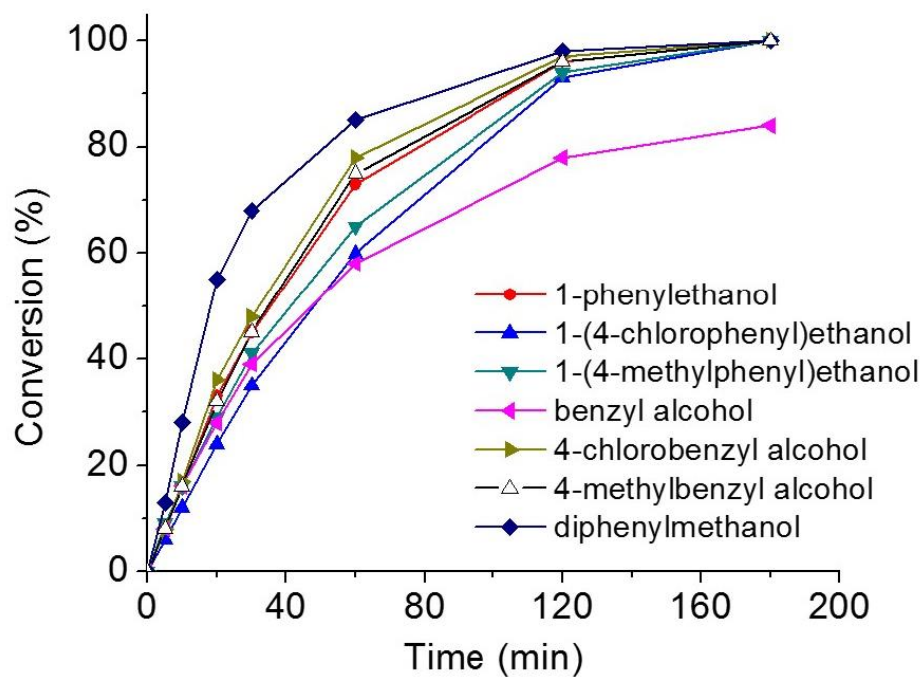


Fig. S11 Time evolution plots of the photooxidation of various *para*-substituted aryl alcohols catalyzed by mesoporous 15% SW₁₁/MES.

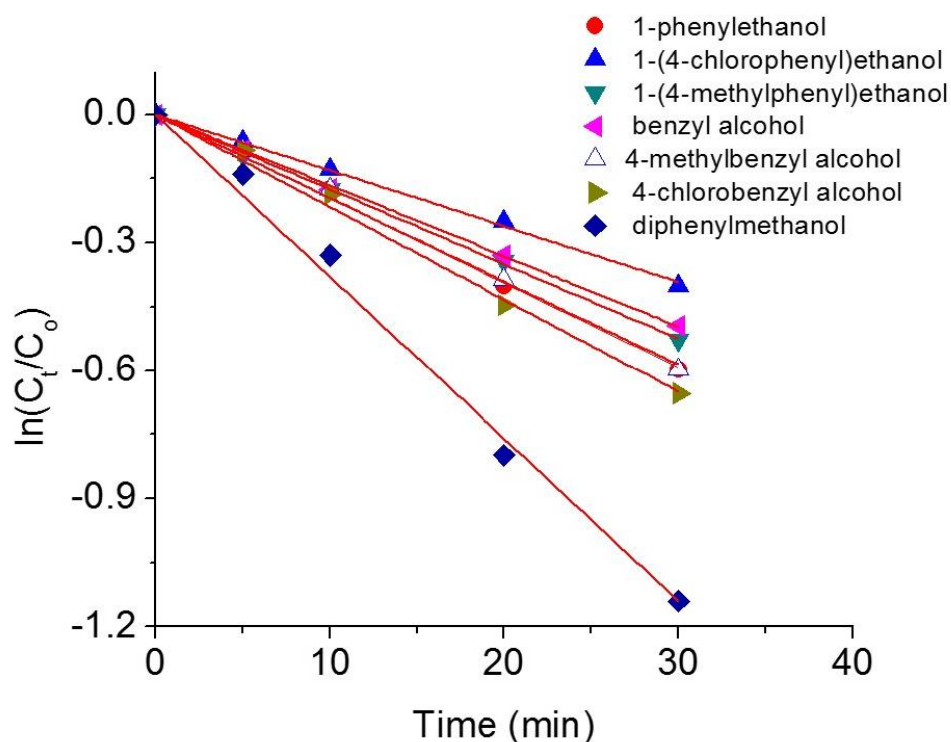


Fig. S12 Kinetic profiles (C_0 , C_t are the initial and final (after time t) molar concentrations of substrate, respectively) of the photooxidation of various *para*-substituted aryl alcohols catalyzed by mesoporous 15% SW₁₁/MES. The corresponding red lines are fit to the data.

References

- 1 A. Téze and G. Hervé, *J. Inorg. Nucl. Chem.*, 1977, **39**, 999.
- 2 R. Zhang and C. Yang, *J. Mater. Chem.*, 2008, **18**, 2691; P. Judeinstein, C. Deprun and L. Nadjo, *J. Chem. Soc., Dalton Trans.*, 1991, **8**, 1991.
- 3 D. Zhao, Q. Huo, J. Feng, B. F. Chmelka, G. D. Stucky, *J. Am. Chem. Soc.*, 1998, **120**, 6024.
- 4 J. Kim, A. A. Gewirth, *Langmuir*, 2003, **19**, 8934.